Molecular beam epitaxy in the presence of phase separation

François Léonard, Mohamed Laradji, and Rashmi C. Desai
Department of Physics, University of Toronto, Toronto, Ontario, Canada M5S 1A7
(Received 19 July 1996)

Experiments have shown that phase separation during the growth of solid films by molecular beam epitaxy (MBE) is a phenomenon seen in a variety of systems. We study a MBE process where two types of particles are deposited simultaneously, and where the interatomic potential energy leads to phase separation. From a microscopic point of view, we describe the system with a solid-on-solid model augmented by an Ising model to represent the phase separation. Monte Carlo simulations of this model show that for low deposition rates, a lamellar pattern emerges in the bulk, with a modulation parallel to the growth plane. We show how the temperature and the deposition rate can be used to tailor the wavelength of the modulation. The effects of the phase separation on the surface morphology create a modulation consisting of steps or grooves at the interface between surface domains, which can be seen in the height-height correlation function and in the surface width. The temperature dependence of the surface width at fixed deposition rate is also presented. [S0163-1829(97)09104-2]

I. INTRODUCTION

Molecular beam epitaxy (MBE) is a process by which particles are deposited on a surface through a directed beam. Technologically, MBE is an important procedure used in the growth of thin solid films. Examples of applications include photovoltaic devices, optoelectronic microsensors, insulator layers, and Bragg reflectors.[1] The MBE growth technique is based on the fact that surface diffusion is an activated process. Particles diffuse on the surface and overcome potential energy barriers with probability proportional to $\exp(-\Delta E/k_BT)$. To successfully grow flat epilayers, the temperature T has to be high, such that atoms have a large probability of finding the minimum energy configuration. However, this process is hindered by the incoming flux of particles. For example, a particle that is not in a minimum energy state can be covered by an incoming particle. The implication of this nonequilibrium growth is that the surface reaches a steady state where the width is saturated but the surface is not at equilibrium. Experimentally then, it is preferable to have high temperature, slow deposition processes. While the simplest way to grow a layer with MBE is to deposit one type of particle (for example, Si on Si), it has now become necessary to grow more complex films made of different atoms. The usage that one wants to make of the epilayer dictates the growth conditions. This is because multicomponent crystals exhibit phase transformations with temperature. For example,[2] bulk equilibrium studies show that $Si_{1-x}Ge_x$ is homogeneous at high temperatures but it phase separates below a certain critical point. On the other hand, $(GaAs)_{1-x}Ge_{2x}$ always unmixes below the melting point of the mixture. The dynamical process of phase separation can be understood in terms of quenching experiments. There, a mixture of two species is suddenly quenched from the homogeneous phase to a state in the coexistence region of the phase diagram. Because of a thermodynamic instability, domains will form and grow in time, leading eventually to complete phase separation. The approach to this state is usually referred to as spinodal decomposition and is a nonequilibrium dynamical phenomenon.

Experimentally, phase separation during crystal growth can be divided into three categories:[3] (i) lateral phase separation, seen in the substrate plane,[4,5] (ii) vertical phase separation, where the modulation is along the growth direction,[6,7] and (iii) vertical phase separation where the concentration modulation is parallel to the growth plane.[8] In their paper, McDevitt *et al.*[4] studied phase separation in $In_{1-x}Ga_xAs$ epilayers grown by MBE (with a growth rate of 1 μm/hour) and found that two-dimensional phase separation occurs in the growth plane, leading to a concentration modulated structure. In the temperature range 670–780 K, they found that the wavelength of the modulation increases with increasing temperature, which they explained with the surface diffusion of As atoms. In another study,[8] Zn, Se, Mg, and ZnS were deposited simultaneously at temperatures around 530 K to grow thin layers (about 1 μm thick) of (100) $Zn_{1-y}Mg_ySe_{1-x}S_x$ or $ZnSe_{1-x}S_x$. In these systems, phase separation is seen in the (vertical) [011] direction occurring mostly for $x>0.2$, and it is observed that the free surface has a modulation of the order of 400 Å, comparable to the bulk concentration modulation.

Theoretically, MBE in the presence of phase separation is a challenging problem because it combines two unsolved nonequilibrium processes: the steady-state reaching MBE growth and the equilibrium reaching phase separation. In particular, we shall show that the scaling behavior of homoepitaxy is only partially carried over to heteroepitaxy, and that the combination of the two nonequilibrium processes may lead to metastable states in the bulk.

Among the theoretical methods to study MBE is to propose a microscopic Hamiltonian and numerically simulate the system using a Monte Carlo algorithm. This approach is useful because it permits us to focus on certain microscopic interactions, and see their effect on the surface growth. Recently, Siegert and Plischke[9] have simulated MBE using a solid-on-solid (SOS) model that allows the surface to relax. In order to simulate MBE with phase separation, we have used a SOS model augmented by an Ising model to describe the phase separation. The dynamics at the surface and in the bulk are chosen to satisfy detailed balance in the absence of

deposition. As a first step, we have investigated our model in 1+1 dimensions, relevant to experimental systems where the strain is highly anisotropic, and phase separation occurs only in a preferred plane. We are aware of one previous Monte Carlo study of phase separation during film growth.[10] The authors presented results of simulations in 2+1 dimensions *without* fluctuations of the free surface, and with diffusion occurring in a thin surface layer. This leads to phase separated microstructures, with a saturated domain size proportional to $F^{-1/3}$, where F is the deposition rate. Our study extends this work by including and studying the fluctuations of the free surface. We also recover the regime $F^{-1/3}$ and identify a new regime where the domain size is proportional to $F^{-1/4}$ at smaller deposition rates.

Our paper is divided as follows. In Sec. II we describe the model and details of the simulation procedure. In Sec. III we present the results of our Monte Carlo simulations while Sec. IV summarizes our findings and gives an outlook for the future.

II. MODEL

During MBE, evaporation of particles is negligible, and the surface relaxation proceeds through diffusion of material along the surface, due to the large surface diffusion coefficient. Typically, overhangs and incorporation of vacancies in the bulk are neglected, and MBE is modeled by SOS models. The investigations of various SOS models have shown that both in 1+1 and 2+1 dimensions, the simplest realistic discrete model Hamiltonian for MBE of a single type of atom is

$$\mathcal{H}_{\mathrm{SOS}}=\frac{1}{2}E_{\mathrm{SOS}}\sum_{\langle i,j\rangle}|h_i-h_j|^n, \tag{1}$$

where h_i is the discrete height at site i and the sum is over nearest-neighbor sites ($E_{\mathrm{SOS}}>0$). The exponent n is related to the so-called Schwoebel barriers:[11] on a vicinal surface of large terraces separated by steps, particles diffusing on a terrace will be repelled from the downward step, because they have to jump over a potential barrier. This barrier is due to a decrease of the coordination number as the particle passes from the upper terrace to the lower terrace. The $n=1$ model possesses a negative Schwoebel effect producing downhill currents and realistic surface properties. The case $n=2$ has a special symmetry and is not expected to be realistic, while for $n=4$ there is a positive Schwoebel effect that causes instabilities and the formation of large pyramidlike structures. For these reasons, we have chosen to model the surface relaxation in our problem with $n=1$. In this case, $\mathcal{H}_{\mathrm{SOS}}$ is proportional to the number of broken bonds at the surface and thus has a simple physical origin.

The properties of this model have been studied both in 1+1 ($d=1$) and 2+1 ($d=2$) dimensions by Monte Carlo simulations.[9] Most of the surface structural properties can be obtained from the surface structure factor, defined as

$$S_s(\mathbf{k},t)=\langle\hat{h}(\mathbf{k},t)\hat{h}(-\mathbf{k},t)\rangle, \tag{2}$$

where $\hat{h}(\mathbf{k},t)=L^{-d/2}\Sigma_{\mathbf{r}}[h(\mathbf{r},t)-\overline{h}]e^{i\mathbf{k}\cdot\mathbf{r}}$ with $\overline{h}$ the average value of $h(\mathbf{r},t)$, L the linear system size, and the angular brackets denote an average over independent initial conditions. The surface structure factor follows a simple scaling form,

$$S_s(\mathbf{k},t)=k^{-\gamma}s(k^z t), \tag{3}$$

with the exponents obeying a hyperscaling relation $\gamma=z$ and being equal to 2. Thus during MBE growth, a unique length scale, ξ, emerges and obeys the power law

$$\xi\sim t^{1/z}. \tag{4}$$

The width of the interface, W, defined through the relation

$$W^2(L,t)=\left(\frac{L}{a}\right)^{-d}\sum_{\mathbf{r}}\langle[h(\mathbf{r},t)-\overline{h}]^2\rangle=a^d\sum_{\mathbf{k}}S_s(\mathbf{k},t) \tag{5}$$

(a is the lattice constant), thus follows a power law in time, $W\sim t^{\beta}$ with $2\beta=(\gamma-d)/z$ until saturation is reached, beyond which the saturated width behaves as $W\sim L^{\zeta}$ with $\zeta=\frac{1}{2}$ for $d=1$ and $\zeta=0$ for $d=2$. Prior to saturation, $W\sim\xi^{\zeta}\sim t^{\zeta/z}$, which leads to the relation $\beta=\zeta/z$. The three relations among the exponents lead to ζ as one independent exponent. The above scaling forms imply that the correlation function scales as

$$G_s(\mathbf{r},t)=\langle[h(\mathbf{r},t)-h(0,t)]^2\rangle=r^{2\zeta}g(r/\xi(t)). \tag{6}$$

Furthermore it was found that the value of ζ is independent of the deposition rate and of the presence of an equilibrium roughening transition.

The above scaling relations and exponents can be reproduced from the Edwards-Wilkinson (EW) equation[12]

$$\partial_t h=\nu\nabla^2 h+F+\eta_h, \tag{7}$$

where F is the deposition rate and η_h its nonconserved fluctuations with second moment D. Indeed, the structure factor is $S_s(\mathbf{k},t)=D/\nu k^2(1-e^{-2\nu k^2 t})$, which gives in the steady state and in 1+1 dimensions $W=(D/\nu)^{1/2}L^{1/2}$.

In the case of heteroepitaxy, one needs to include in the model the interactions between different atomic species. The simplest model capable of describing phase separation in a binary alloy is the Ising model

$$\mathcal{H}_{\mathrm{Ising}}=-\frac{1}{2}E_{\mathrm{Ising}}\sum_{\langle i,j\rangle}\sigma_i\sigma_j, \tag{8}$$

where σ_i is a variable equal to ±1 for an A or B atom, respectively, and the sum is over nearest-neighbor pairs. On a two-dimensional square lattice, the Ising model has a phase transition between a high temperature homogeneous phase and a low temperature two-phase region around $T_c\approx 2.26(E_{\mathrm{Ising}}/k_B)$, k_B being Boltzmann's constant. The dynamical evolution of such a system after a quench from a high temperature to a temperature below T_c is governed by an initial instability and the development of domains, of local order parameter corresponding to that of the two coexisting phases, with average size growing as a power law in time with an exponent $\frac{1}{3}$.[13–15] For MBE, we suppose that the concentration of each atomic type falling on the surface is constant in time, and because of conservation of material, $(hL^d)^{-1}\Sigma_{\mathrm{system}}\sigma_i=$ const. A coarse-grained description of

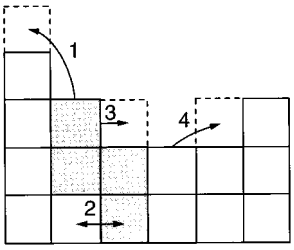

FIG. 1. Monte Carlo moves allowed in the simulations. Processes 1, 3, and 4 are surface diffusions, while process 2 is a bulk exchange.

the phase separation in the Ising model in terms of a continuous variable $\phi(\mathbf{r})$ proportional to the local concentration difference of the two species is the Cahn-Hilliard equation:[16]

$$\partial_t \phi = M\nabla^2(-\phi+\phi^3-\nabla^2\phi)+\eta_\phi, \tag{9}$$

with M the mobility and η_ϕ a conserved thermal noise related to M through a fluctuation-dissipation relation.

We postulate the full Hamiltonian for MBE with phase separation to be

$$\mathcal{H}=\mathcal{H}_{\rm SOS}+\mathcal{H}_{\rm Ising}. \tag{10}$$

There are three parameters entering in our model: $E_{\rm Ising}/E_{\rm SOS}$, $k_BT/E_{\rm SOS}$, and the deposition rate F. In the following, we have set $E_{\rm SOS}$ to 1 and shall refer to $k_BT/E_{\rm SOS}$ as T, while lengths are rescaled by the lattice constant a.

In the simulations, we start with a one-dimensional flat interface of size L, and the space above the substrate is divided in a square lattice with lattice constant $a=1$. A site i from 1 to L is chosen randomly, and a particle is deposited at h_i+1. In the case of a ''critical'' deposition, i.e., $\Sigma_{\rm system}\sigma_i=0$, we choose the type of the freshly landed atom randomly to be ± 1. Then, we randomly visit all of the atoms that have been deposited. If the atom lies on the surface, it is allowed to hop to a nearest-neighbor site on the surface (corresponding to processes 1, 3, and 4 in Fig. 1) with a transition rate

$$w_{i\to j}=\exp\left(-\frac{\Delta\mathcal{H}_{i\to j}}{T}\right), \tag{11}$$

where $\mathcal{H}$ is the Hamiltonian of Eq. (10). This choice for the transition rates ensures that detailed balance is satisfied if the deposition rate is set to zero.[9] If the atom lies in the bulk, we randomly choose a nearest-neighbor site and attempt to exchange the two atoms, as process 2 of Fig. 1 illustrates (this choice for the bulk dynamics conserves the volume fraction). We do not allow exchanges between surface and bulk atoms, and assume periodic boundary conditions along the x direction. The deposition rate F is controlled by the number of sweeps through the surface after each deposition. To model the difference in the diffusion constant on the surface and in the bulk, the number of diffusion attempts (Monte Carlo steps) per deposition event for atoms on the surface is set to n_s, while for atoms in the bulk it is n_b. For $n_b<n_s$ the surface diffusion coefficient is larger than the bulk diffusion coefficient. If E_e is the extra activation energy for an atom in the bulk as compared to an atom at the surface, then the ratio $n_b/n_s\sim\exp(-E_e/k_BT)$. In our simulations, we have kept the ratio $n_b/n_s=0.01$ fixed. The deposition rate F in time units of Monte Carlo steps is $F=1/n_s$.

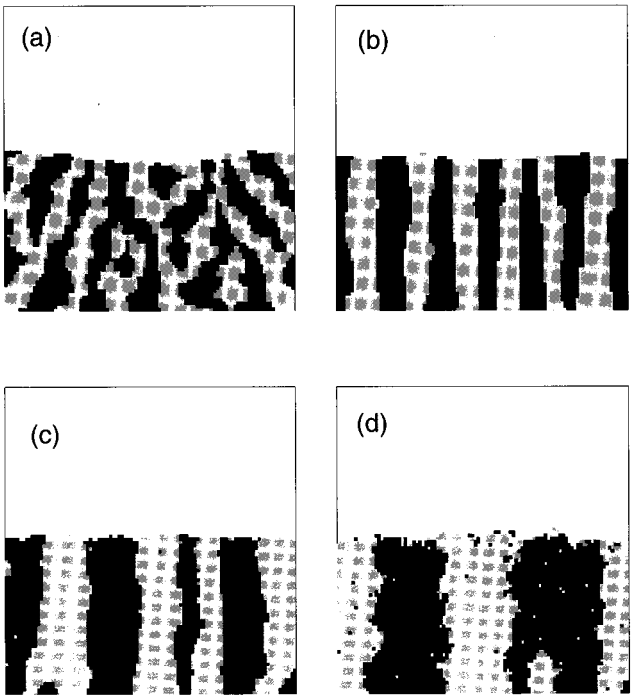

FIG. 2. Top 50 layers after deposition of 200 layers for $n_s=100$, $E_{\rm Ising}=1$, and $T=$ (a) 0.2, (b) 0.5, (c) 1.0, (d) 1.6. Only a partial section of size 100 of the $L=200$ system is shown.

III. RESULTS

We have simulated our model for systems of size $L=200$, for various values of the Ising and SOS interactions and with different deposition rates and temperatures. If $\varepsilon(\sigma_i,\sigma_j)$ represents the interaction energy between nearest-neighbor atoms i and j, and if we identify a vacancy with $\sigma=0$, the energies in our model are $\varepsilon(1,1)=\varepsilon(-1,-1)=-E_{\rm Ising}$, $\varepsilon(1,-1)=\varepsilon(-1,1)=E_{\rm Ising}$, and $\varepsilon(\pm 1,0)=E_{\rm SOS}$. In the case where $E_{\rm Ising}>2E_{\rm SOS}$, processes 3 (detachment from islands) and 4 of Fig. 1 will spontaneously occur because they lower the energy, thereby creating very rough surfaces. With our choice for the Hamiltonian (and large $E_{\rm Ising}$), process 4 will always reduce the energy, independently of the depth of the groove, leading to columnar structures.

A. Effects of temperature

Figure 2 shows the top 50 layers after deposition of 200 layers for temperatures below the critical temperature, with the deposition rate fixed at $n_s=100$. We found that if we set the bulk diffusion to zero, the same kind of lamellar patterns appear, implying that the phase separation occurs at the surface. For temperatures above the critical temperature, the atoms are homogeneously mixed, in agreement with annealing experiments.[3] Below T_c, the atoms form domains at the surface that are buried as the film grows. New deposited atoms then diffuse on top of the surface, which now contains con-

centration gradients, and will tend to stay on top of lamellae that minimize the bonding energy. Iteration of this idea produces stripes that extend from the substrate to the free surface. When the bulk interfaces are straight, they do not decay and are metastable. [In fact, $\phi=\tanh(x/\sqrt{2})$ is a one-dimensional steady-state solution of Eq. (9) without thermal noise]. For the lamellar bulk configurations where the concentration interfaces are rough, reducing the temperature after the deposition process would quench in the morphology. On the other hand, this roughness could be decreased by the local straightening of the interfaces by the chemical potential gradients as time proceeds, leading to flat interfaces. Which of these two processes is useful in practice depends on the application. For example, in Ref. 17, it has been shown that the interface roughness in semiconductor superlattices leads to quantum phase-coherent backscattering which localizes the electrons and increases the magnetoresistance.

As Fig. 2 illustrates, the pattern wavelength depends strongly on the temperature. At low temperatures, the diffusion length is small, and the atoms sample the surface only locally and stick. For example, at $T=0$, a move occurs only if $\Delta\mathcal{H}\leqslant 0$, i.e., attachment to islands, downward jumps, or diffusion on a flat surface. This creates small domains, and an interconnected bulk domain structure. At the top surface, steps form at the domain boundaries, and sometimes arrange themselves in step trains [Fig. 2(a)]. As the temperature is increased two effects come into play. First, the increase in the diffusion length causes the lamellar thickness, λ, to increase. Second, surface atoms acquire enough thermal energy to overcome the energy barriers at the surface domain boundaries, and diffuse to the top of stripes of opposite concentration, leading to a larger bulk miscibility than that of the equilibrium mixture. We stress that at low temperatures a newly deposited atom diffuses to the nearest favorable lamellae and stays confined to the top of this stripe. The diffusion length is then only of the order of λ. Because the one-component model leads to self-affine surfaces, the fact that the atoms are confined within λ does not drastically affect the value of the surface width, except for corrections at surface domain boundaries.

The wavelength of the bulk pattern is an important quantity to measure as a function of the temperature. In order to calculate the thickness of the stripes, we have computed the concentration structure factor $S_\sigma(k)=L^{-1}\langle\sigma_k\sigma_{-k}\rangle$ in the direction parallel to the growth plane, 25 sites below the average steady-state height. The peak in $S_\sigma(k)$ represents the modulation period. A measure of the lamellar thickness, λ, can be obtained from twice the first zero of the correlation function $G_\sigma(x)=L^{-1}\Sigma_k S_\sigma(k)\cos(kx)$. Figure 3 shows the correlation function for the temperatures of Fig. 2. The periodic structure is apparent in the oscillations of the correlation function about zero, and as the temperature is increased, spatial correlations extend further along the direction parallel to the growth plane.

The temperature dependence of λ is plotted in Fig. 4. As a general trend, λ increases at low temperatures, reaches a maximum, and decreases as T_c is approached. This behavior can be explained by considering the motion of interfaces between ordered domains on the surface. The steady-state wavelength is related to the velocity of the moving interfaces times the typical time scale between monolayer completion.

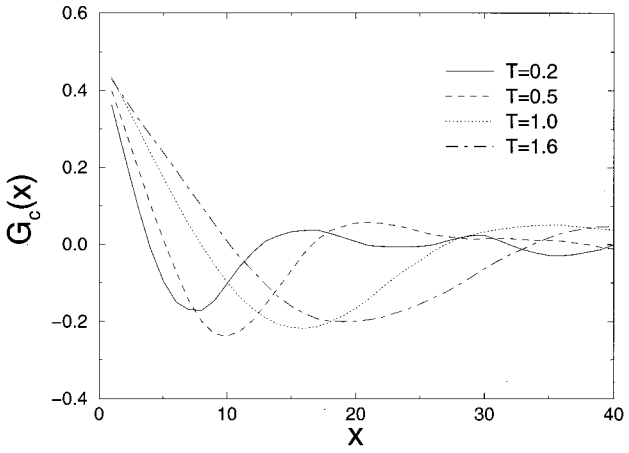

FIG. 3. Bulk correlation function in the direction parallel to the growth plane for the parameters of Fig. 2.

The interface velocity (and hence λ) is proportional to the surface tension and the diffusion coefficient. The surface tension is constant at low temperatures and decreases towards zero as the critical point is approached, while the diffusion coefficient should have an Arrhenius form. These two effects conspire to give a maximum in $\lambda(T)$. In addition, the shape of this curve shows a shoulder around $T=0.6$, which can be associated with the behavior of the surface width, which we discuss next.

We find that the width has a nonmonotonic temperature dependence, as shown in Fig. 5. As the temperature is increased from zero, the width (solid circles) decreases linearly with T, reaches a minimum, and then starts to increase as T^2. This minimum occurs around the same temperature where $\lambda(T)$ has a shoulder in Fig. 4. For comparison, we show in Fig. 5 the width (W_{SOS}) when only one kind of atom is deposited. In contrast to heteroepitaxy, W_{SOS} increases roughly as T for $T>0.6$. Our understanding of the temperature dependence of the interface width is as follows: at low temperatures, atoms form thin lamellae, and the energy barriers at the A-B interfaces keep the atoms on top of a favorable stripe (i.e., same type). This creates steps at the lamellar

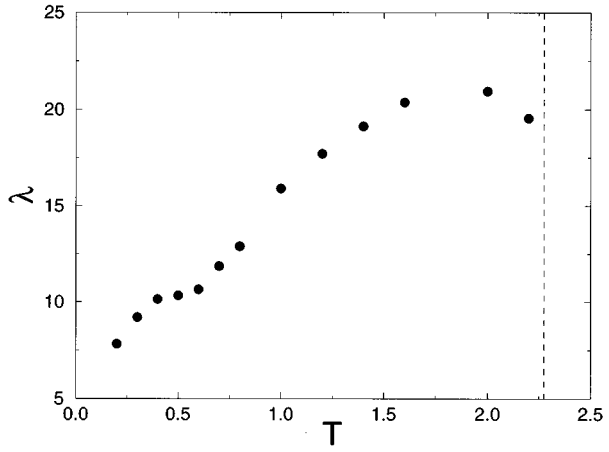

FIG. 4. Lamellar thickness as a function of temperature for $n_s=100$. The vertical dashed line corresponds to the critical temperature for the Ising model on a square lattice.

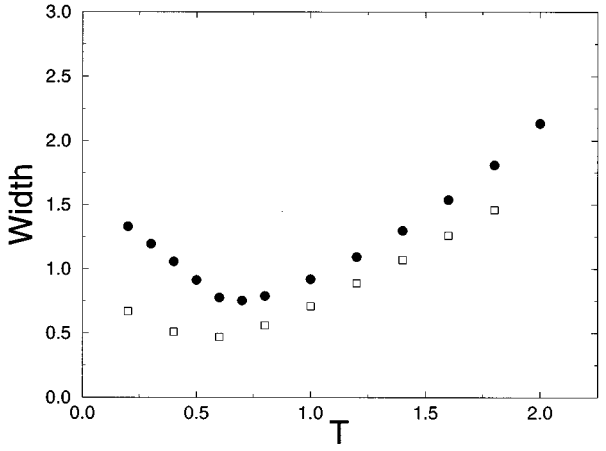

FIG. 5. Temperature dependence of the surface width. The solid circles are for MBE with phase separation, while the open squares correspond to single-component MBE.

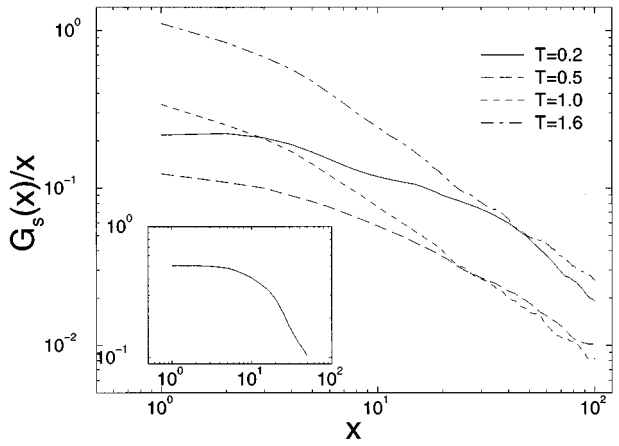

FIG. 6. Scaling function for the surface correlation function for temperatures above and below the width minimum. The inset is the scaling function for single-component MBE.

interfaces and gives rise to a width larger than W_{SOS}. Since the number of interfaces decreases with temperature, the width also decreases, and does so faster than W_{SOS}. With the assumption that the system is composed of pure lamellae of thickness λ, the average size of the steps can be evaluated from $h_i = h_i^{\mathrm{SOS}} + \Delta h\, \delta_{i,n\lambda/a}$, where n is an index labeling the location of the surface domain interfaces. This gives $\Delta h = \sqrt{\lambda}(W^2 - W_{\mathrm{SOS}}^2)^{1/2}$, and from our data points, we find that Δh is of order 1 and decreases in the range $0.2 < T < 0.6$. There are two possible explanations for this: either the size of the steps is temperature dependent, or the effect on the neighbor sites that we have neglected has to be taken into account (this is more important when λ is small). At high temperatures, the atoms can jump over the potential energy barriers at the surface A-B interfaces, leading to a mixing at the top of these stripes, thereby decreasing the surface tension and thus causing the width to increase rapidly with T in Fig. 4. This enhanced diffusion at $T > 0.6$ is also responsible for the sudden increase of λ with T. The high temperature behavior can be explained in terms of a continuous equation that includes both the EW term and the surface tension contribution:

$$\partial_t h = \nu \nabla^2 h + \Lambda \gamma \nabla^4 h + \eta_c + \eta_{\mathrm{nc}} \tag{12}$$

with η_c a conserved thermal noise with second moment $\langle \eta_c(x,t)\, \eta_c(x',t') \rangle = -2\Lambda k_B T \nabla^2 \delta(x-x')\, \delta(t-t')$, and η_{nc} a nonconserved beam noise of strength D. In this equation, Λ is a kinetic coefficient and γ is the surface stiffness. The steady-state structure factor can be easily calculated, and is given by

$$S_s(k) = \frac{D + \Lambda k^2 k_B T}{\nu k^2 + \Lambda \gamma k^4}, \tag{13}$$

which reduces to $S_s(k) = \Lambda k_B T (\nu + \Lambda \gamma k^2)^{-1}$ in the limit of small D and large T. From this expression, we obtain the surface width

$$W^2 = \frac{\Lambda k_B T}{\sqrt{\Lambda \gamma \nu}} \left[\arctan\left(\sqrt{\frac{\Lambda \gamma}{\nu}} \frac{2\pi}{a} \right) - \arctan\left(\sqrt{\frac{\Lambda \gamma}{\nu}} \frac{2\pi}{L} \right) \right]. \tag{14}$$

When the system size is large and the lattice constant is small, the surface width becomes $W \sim (\Lambda k_B T / \sqrt{\Lambda \gamma \nu})^{1/2}$. In the homoepitaxial case, γ is constant, and the temperature dependence is buried in ν and Λ. In the case of heteroepitaxy with phase separation, we expect the temperature dependence of ν and Λ to remain roughly the same, while γ acquires a temperature dependence due to the diffusion effect discussed earlier. Because γ decreases with temperature, the overall effect is to cause the width to increase faster than in homoepitaxy.

The shape of the surface can be described by computing the surface correlation function $G_s(r)$ as defined in Eq. (6). As Fig. 6 indicates, the correlation function is qualitatively different for temperatures above and below the minimum in the surface width. For large distances, $r^{-1} G_s(r)$ for $T = 1.0$ and $T = 1.6$ decays as r^{-1}, consistent with the behavior of the one-component SOS model (see inset). However, at small distances, these two functions are not constant. The true height-height correlation is equal to $2W^2 - G_s(r)$, which means that the height loses correlation faster for $T > 0.6$. This is in agreement with the previous statement that thermal fluctuations become important in this regime. Because the interface width is of order 1, the effects of the domain interfaces on the surface shape are not apparent in the surface correlation function or the structure factor, although at low temperatures, extra steps are obviously seen in the configurations, and at high temperatures, grooves and steps are more often seen at those interfaces. To clarify this, we simulated the system at large values of E_{Ising}. As Fig. 7 illustrates, grooved states are now more apparent in the configurations. In the case where $E_{\mathrm{Ising}} = 1.9$, grooves are found to occur at the surface domain interfaces, with a saturated depth of 3–4 atoms, while the other surface features (roughness) are one atom high. For $E_{\mathrm{Ising}} = 4$, it becomes energetically favorable under certain conditions for the system to incorporate vacancies between stripes of opposite concentration, creating very thin and deep crevices. Such large modulations of the surface are now visible in the surface structure factor (Fig. 7). The peak at $q = 0$ represents the usual fluctuations that lead to self-affine surfaces (that is, of the EW form), while the peak at $q \neq 0$ represents the surface modulation. Note that as time

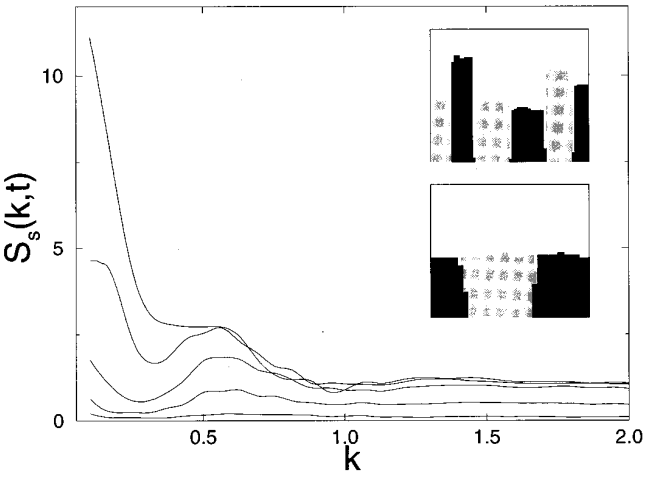

FIG. 7. Time evolution of the surface structure factor for $E_{\text{Ising}}=4$. Curves from bottom to top correspond to time = 20, 30, 40, 60, and 100 monolayers. The peak at $q=0$ is typical of homoepitaxy, while the peak at nonzero q represents the surface modulation. In the inset, the top configuration is typical of this regime, whereas the bottom configuration shows grooves as seen when $E_{\text{Ising}}=1.9$.

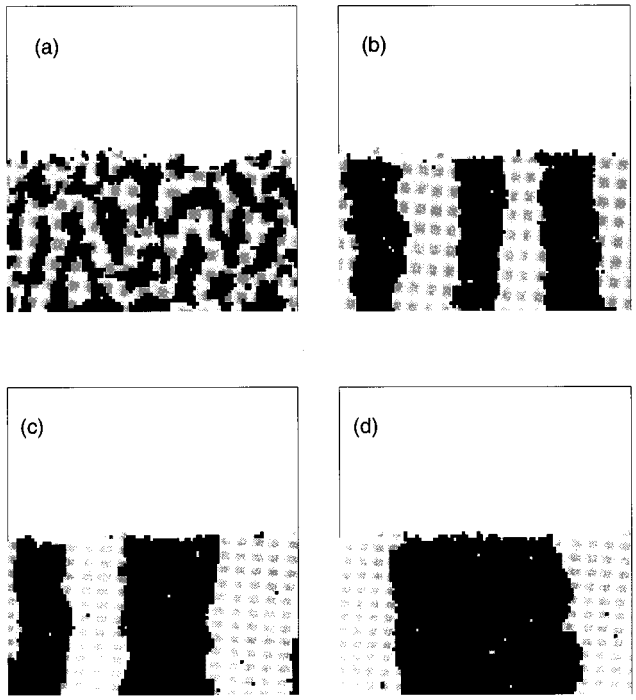

FIG. 8. Typical configurations for $T=1.2$ and $n_s=$ (a) 1, (b) 100, (c) 400, (d) 1000. The top 50 layers and only a partial section of size 100 of the $L=200$ system is shown.

increases, the divergence at $q=0$ overwhelms the modulation peak. As discussed earlier, when the Ising interaction is not as large, the surface saturates rapidly, and the peak in the surface structure factor is not as clear. The extreme roughness of the surface for large E_{Ising} has been seen experimentally during codeposition of Al-Ge thin films.[18] In particular, phase separation is found at the surface and in the bulk, with the Al domains forming large mounds of height 0.25 μm. Whether such deformations of the surface are due to the effects we are reporting here or due to elastic effects remains to be explored.

B. Effects of the deposition rate

Although the lamellar wavelength can be controlled by appropriately choosing the temperature, this also leads to wandering lamellae at low temperatures or rough lamellar interfaces at high temperatures. One can alternatively control the pattern wavelength by varying the deposition rate. Qualitatively, the effects of the deposition rate are shown in Fig. 8, from which it is clear that a decrease in the deposition rate ($F=1/n_s$) increases λ, since the atoms have a longer time to sample the surface before being covered. Also, at larger rates, the surface roughness increases. In Fig. 9, we plot the lamellar thickness as a function of the deposition rate at fixed temperature. Our data are well described by $\lambda \sim F^{-x}$ (where $F \sim 1/n_s$) with $x=1/3$ for low deposition rates, and $x=1/4$ for moderate deposition rates. For $1/n_s > 0.1$, the bulk consists of an interconnected structure, suggesting a critical growth rate above which the film is homogeneous.

These results can be explained in terms of a coarse-grained description of the system. The height of the surface is represented by a single-valued continuous variable $h(\mathbf{x})$ obtained by coarse-graining the microscopic discrete height, and the local concentration of the two species is represented by the continuous order parameter $\phi(\mathbf{r})$. The dynamical equation describing the order parameter at the surface, $\phi(\mathbf{x},h(\mathbf{x}))$, is given by[19]

$$\frac{\partial \phi}{\partial t} = M_S \nabla_S^2[-\phi+\phi^3-\nabla^2\phi]+\Phi(\phi_0-\phi)+\eta_{\phi_S}, \tag{15}$$

where M_S is the surface mobility. The noise η_{ϕ_S} in Eq. (15) is nonconserved since it represent the fluctuations of the con-

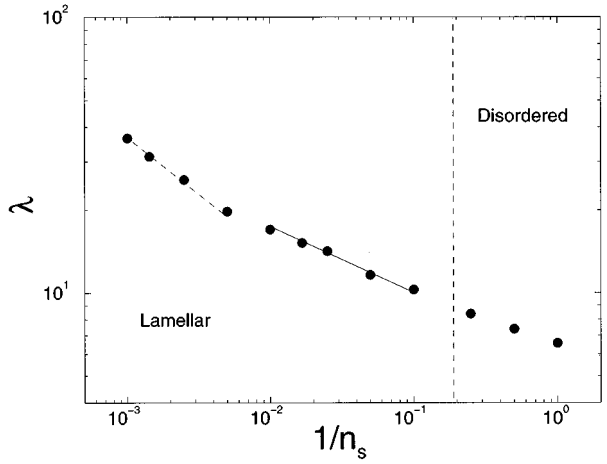

FIG. 9. Thickness of the lamellae as a function of the deposition rate at $T=1.2$. The solid (dashed) line has slope $-1/4$ ($-1/3$). The vertical line represents roughly the transition between the lamellar and the disordered regimes.

centration in the beam. The operator ∇_S^2 ensures that the diffusion is along the surface and contains nonlinearities in ∇h due to the non-Euclidian nature of the surface. The linear term in ϕ coupled to the beam concentration deposition rate, Φ, has been proposed before.[20] This contribution can be obtained as follows: we can write $\phi(t+\Delta t)=\phi(t)+R\Delta t$, where R represents the concentration of material falling on the surface per unit time. R can be expanded around the average value of the order parameter, ϕ_0: $R(\phi)=R(\phi_0)+\Phi(\phi_0-\phi)$. This equation simply states that the order parameter has a tendency to flow towards ϕ_0. The coefficient Φ is proportional to the velocity at which the solid-vacuum interface is growing.

At early times of the deposition, the system is homogeneous, and we can therefore expand ϕ around its mean value, $\phi=\phi_0+\delta\phi$, and neglect the nonlinearities due to the surface shape in Eq. (15). The dispersion relation for $\delta\phi$ is then $\Omega(q)=M_S q^2(1-3\phi_0^2-q^2)-\Phi$, which is positive in the band of wave vectors,

$$(1-3\phi_0^2)-\sqrt{(1-3\phi_0^2)^2-4\frac{\Phi}{M_S}}<2q^2 < (1-3\phi_0^2)+\sqrt{(1-3\phi_0^2)^2-4\frac{\Phi}{M_S}} \quad (16)$$

if

$$\Phi < \Phi_c = \frac{1}{4}M_S(1-3\phi_0^2)^2. \quad (17)$$

Hence, for values of Φ below Φ_c, there is an instability that causes fluctuations in ϕ to be amplified. The expression for the critical deposition rate, Φ_c, shows that phase separation will occur if the following conditions are met: first, for deposition rates smaller than Φ_c, second, if $\phi_0<1/\sqrt{3}$, and third, if the temperature is such that M_S satisfies Eq. (17). In the steady state, Eq. (15) predicts a periodic solution with wavelength $\lambda\sim\Phi^{-1/3}+O(1)$ far from the onset of instability, and $\lambda^{-4}=\Phi+O(\epsilon^4)$ with $\epsilon^2=\Phi_c-\Phi$ near the onset of instability.[19]

IV. CONCLUSION

In this paper, we have considered the growth of thin solid films by molecular beam epitaxy. We considered the growth of multicomponent films, where the ground-state energy favors phase separation. During the growth process, two phenomena attracted our attention. First, we were interested in surface roughening, whereby the beam fluctuations are transformed into fluctuations of the surface height, and typically leads to self-affine surfaces. Second, the growth of correlated domains due to the nature of the chemical potential (phase separation) was considered. The interplay between these two processes is the central theme of this work. Our Monte Carlo simulations demonstrated three important aspects seen in experimental systems: above a critical temperature, the films are homogeneous; the wavelength of the concentration modulation increases with temperature; phase separation does not occur by bulk diffusion. Furthermore, our data indicate that the width of the free surface is only slightly larger when phase separation is present. The characteristics of the surface were also analyzed using the structure factor and the correlation function. The self-affinity of the surface is destroyed by the concentration gradients, and this was explained by the presence of steps and grooves at the interface between domains. The evidence for this comes from the behavior of the interface width as a function of temperature, from the form of the surface correlation function, and by simulation results at high values of the ratio $E_{\rm Ising}/E_{\rm SOS}$.

This work is a first attempt to explain phase separation during MBE. The application of our theory and results to specific systems requires fine tuning of the parameters in our models. Also, new insight could be obtained by introducing additional important effects. Among these, the inclusion of elastic interactions (stress and strain) is the next logical step, as well as considerations of systems in $2+1$ dimensions.

ACKNOWLEDGMENTS

This work was supported by the Natural Sciences and Engineering Research Council of Canada. F.L. was supported by the Ontario Graduate Scholarships from the Province of Ontario, and le Fonds pour la Formation de Chercheurs et l'Aide à la Recherche de la Province du Québec.

[1] See, for example, *The Technology and Physics of Molecular Beam Epitaxy*, edited by E. H. C. Parker (Plenum Press, New York, 1985).

[2] M. Laradji, D. P. Landau, and B. Dunweg, Phys. Rev. B **51**, 4894 (1995).

[3] A. Zunger and S. Mahajan, *Handbook on Semiconductors*, 2nd ed. (Elsevier, Amsterdam, 1993), Vol. 3.

[4] T. L. McDevitt, S. Mahajan, D. E. Laughlin, W. A. Bonner, and V. G. Keramidas, Phys. Rev. B **45**, 6614 (1992).

[5] S. N. G. Chu, S. Nakahara, K. E. Strege, and W. D. Johnston, Jr., J. Appl. Phys. **57**, 4610 (1985).

[6] P. M. Petroff, A. Y. Cho, F. K. Reinhart, A. C. Gossard, and W. Wiegmann, Phys. Rev. Lett. **48**, 170 (1982).

[7] I. T. Ferguson, A. G. Norman, B. A. Joyce, T. Y. Seong, G. R. Booker, R. H. Thomas, C. C. Phillips, and R. A. Stradling, Appl. Phys. Lett. **59**, 3324 (1991).

[8] G. C. Hua, N. Otsuka, D. C. Grillo, J. Han, L. He, and R. L. Gunshor, J. of Cryst. Growth **138**, 367 (1994).

[9] M. Siegert and M. Plischke, Phys. Rev. E **50**, 917 (1994); Phys. Rev. Lett. **68**, 2035 (1992); J. Phys. I **3**, 1371 (1993).

[10] C. D. Adams, D. J. Srolovitz, and M. Atzmon, J. Appl. Phys. **74**, 1707 (1993).

[11] J. Villain, J. Phys. I **3**, 19 (1991).

[12] S. F. Edwards and D. R. Wilkinson, Proc. R. Soc. London, Ser. A **381**, 17 (1982).

[13] C. Roland and M. Grant, Phys. Rev. Lett. **60,** 2657 (1988).

[14] T. M. Rogers, K. R. Elder, and R. C. Desai, Phys. Rev. B **37**, 9638 (1988).

[15] J. G. Amar, F. E. Sullivan, and R. D. Mountain, Phys. Rev. B **37**, 196 (1988).
[16] J. D. Gunton, M. San Miguel, and P. Sahni, in *Phase Transitions and Critical Phenomena*, edited by C. Domb and J. L. Lebowitz (Academic, London, 1983), Vol. 8.
[17] B. Laikhtman and D. Menashe, Phys. Rev. B **52**, 8974 (1995).
[18] C. D. Adams, M. Atzmon, Y.-T. Cheng, and D. J. Srolovitz, J. Mater. Res. **7**, 653 (1992).
[19] F. Léonard and R. C. Desai (unpublished).
[20] M. Atzmon, D. A. Kessler, and D. J. Srolovitz, J. Appl. Phys. **72**, 442 (1992).